



Audio Engineering Society Convention Paper

Presented at the 131st Convention
2011 October 20–23 New York, USA

This Convention paper was selected based on a submitted abstract and 750-word precis that have been peer reviewed by at least two qualified anonymous reviewers. The complete manuscript was not peer reviewed. This convention paper has been reproduced from the author's advance manuscript without editing, corrections, or consideration by the Review Board. The AES takes no responsibility for the contents. Additional papers may be obtained by sending request and remittance to Audio Engineering Society, 60 East 42nd Street, New York, New York 10165-2520, USA; also see www.aes.org. All rights reserved. Reproduction of this paper, or any portion thereof, is not permitted without direct permission from the Journal of the Audio Engineering Society.

Local Sound Field Synthesis by Virtual Acoustic Scattering and Time-Reversal

Sascha Spors, Karim Helwani, and Jens Ahrens

Deutsche Telekom Laboratories, Technische Universität Berlin, Ernst-Reuter-Platz 7, 10587 Berlin, Germany

Correspondence should be addressed to Sascha Spors (Sascha.Spors@telekom.de)

ABSTRACT

Sound field synthesis techniques, like Wave Field Synthesis and near-field compensated higher order Ambisonics, aim at synthesizing a desired sound field within an extended area using an ensemble of individually driven loudspeakers. Local sound field synthesis techniques achieve an increased accuracy within a restricted local listening area at the cost of stronger artefacts outside. This paper proposes a novel approach to local sound field synthesis that is based upon the scattering from a virtual object bounding the local listening area and the time-reversal principle of acoustics. The physical foundations of the approach are introduced and discussed. Numerical simulations of synthesized sound fields are presented, as well as a comparison to other published methods.

1. INTRODUCTION

Sound field synthesis (SFS) techniques aim at the synthesis of a sound field within an extended area using an ensemble of individually driven loudspeakers. It is generally assumed that an improved synthesis in the physical sense results in favorable perceptual properties, e.g. the improvement of the sweet-spot limitation [1] known from stereophonic approaches. Well established sound field synthesis techniques are for instance Wave Field Synthesis (WFS) [2, 3, 4], near-field compensated higher order

Ambisonics (NFC-HOA) [5, 6, 7] and the Spectral Division Method (SDM) [8]. However, all off these techniques suffer from limitations when practically implemented. One major limitation is that the synthesis accuracy is limited by the number of loudspeakers employed in a particular setup. Currently available setups used for WFS or NFC-HOA do not allow the accurate synthesis for an extended area for the full audio bandwidth of 20 kHz. Spatial sampling artifacts arise typically above 1-2 kHz. Since the underlying hearing mechanisms for synthetic sound fields are not clear at the current state of knowledge,

it is also not exactly known which level of physical accuracy is required. For WFS it is for instance known that these artifacts may lead to perceivable coloration of the virtual source [9]. An increase in synthesis accuracy for a given setup is desirable in practical situations.

In the past, several local sound field synthesis techniques (LSFS) have been proposed [10, 11, 12, 13, 14]. These techniques aim at an increased synthesis accuracy within a smaller (local) area than using the traditional approaches to sound field synthesis with a given loudspeaker setup. The increase in accuracy comes at the cost of stronger artifacts outside of the local listening area. Such approaches are useful when the listener positions are restricted to a predefined region of interest.

This paper presents a novel approach to LSFS. It has been noted that the problem of synthesizing a sound field within an extended area using a distribution of loudspeakers (interpreted as single layer potential) can be interpreted as a scattering problem [15, 16]. The basic concept of the proposed approach is to control the sound field at the boundary of the local listening area such as when a scattering object would be present there. It can be shown, based on considerations of the according boundary conditions, that the sound field impinging on a scattering object is apparent inside the scattering object without any disturbance. Instead of explicitly solving the underlying physical problem in order to compute the loudspeaker driving signals, the reciprocity principle of the wave equation is exploited. We show that the desired sound field evolves inside the virtual scattering object when a time-reversed copy of the sound field scattered from the virtual object is synthesized by a loudspeaker array.

The paper is organized as follows: In Section 2 traditional SFS techniques are briefly reviewed, Section 3 introduces the proposed approach, results are shown in Section 4 and finally some conclusions are given in Section 5.

2. SOUND FIELD SYNTHESIS

2.1. Problem Statement

Sound field synthesis techniques aim at the synthesis of a desired sound field within an extended area using an ensemble of individually driven loudspeakers. Without loss of generality it is assumed that

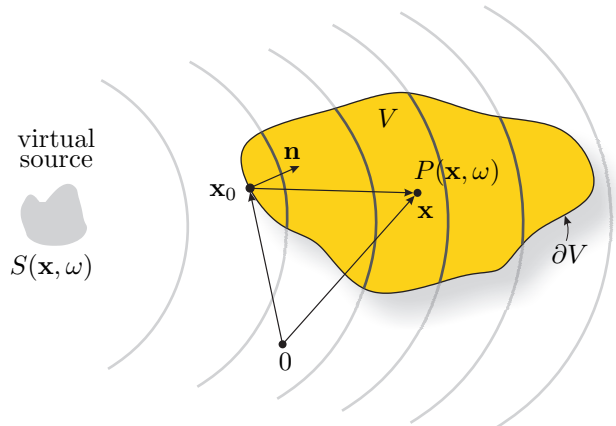


Fig. 1: Illustration of the geometry used to discuss the physical foundations of sound field synthesis.

the desired sound field $S(\mathbf{x}, \omega)$ can be represented by a distribution of virtual sources located outside of the desired listening area V . The physical background of SFS is discussed by replacing the ensemble of loudspeakers by a spatially continuous distribution of secondary sources located on the boundary of the listening area ∂V . This theoretical viewpoint has the benefit that the spatial sampling can be investigated and discussed explicitly. The geometry of the problem setup is illustrated in Figure 1. The synthesized sound field $P(\mathbf{x}, \omega)$ is given as

$$P(\mathbf{x}, \omega) = \oint_{\partial V} D(\mathbf{x}_0, \omega) G(\mathbf{x} - \mathbf{x}_0, \omega) dA_0, \quad (1)$$

where $\omega = 2\pi f$ denotes the radial frequency, $D(\mathbf{x}_0, \omega)$ a frequency and position dependent weight of the secondary source (driving signal), $G(\mathbf{x} - \mathbf{x}_0, \omega)$ the transfer function of the secondary source placed at position \mathbf{x}_0 to the point \mathbf{x} and dA_0 stands for a surface element for integration. A suitable model for $G(\mathbf{x} - \mathbf{x}_0, \omega)$ is the acoustic point source (monopole) since it can be approximated reasonably well by available loudspeakers.

The driving signal $D(\mathbf{x}_0, \omega)$ has to be chosen such that the synthesized sound field $P(\mathbf{x}, \omega)$ equals the sound field of the virtual source $S(\mathbf{x}, \omega)$ within the listening area V . For this purpose, (1) has to be solved with respect to the driving signal $D(\mathbf{x}_0, \omega)$ for $P(\mathbf{x}, \omega) = S(\mathbf{x}, \omega)$. The two most relevant techniques to derive the driving signal are discussed briefly in the following two subsections.

2.2. Explicit Solution

Equation (1) constitutes an integral equation that has to be solved with respect to the driving signal $D(\mathbf{x}_0, \omega)$. According to operator theory [17, 18, 19], the integral in (1) can be understood as a (compact) Fredholm operator of zero index. The general solution is given by expanding the operator and the virtual sound field into a series of orthogonal basis functions and comparison of coefficients. The driving signal is then given as [19]

$$D(\mathbf{x}, \omega) = \sum_{\nu=0}^{\infty} \frac{\tilde{S}(\nu, \omega)}{\tilde{G}(\nu, \omega)} \psi_{\nu}(\mathbf{x}), \quad (2)$$

where $\psi_{\nu}(\mathbf{x})$ denotes a set of orthogonal basis functions, and $\tilde{S}(\nu, \omega)$ and $\tilde{G}(\nu, \omega)$ the projections of the sound field of the virtual source and secondary sources onto the basis functions, respectively.

It is known from operator theory that the solution of (1) is not unique at the eigenfrequencies of the interior homogeneous Dirichlet problem and might be ill-conditioned in practice. In theory, suitable basis functions can be found for arbitrary simply connected domains V with smooth boundaries. In the literature, analytic basis functions and solutions are only available for regular geometries like circles or spheres. Here surface spherical harmonics provide a suitable set of basis functions. The explicit solution of (1) for circular and spherical secondary source distributions is the basis of NFC-HOA, and for linear and planar distributions the basis of the SDM.

2.3. Implicit Solution

An implicit solution to the synthesis equation (1) is given by interpreting the secondary source distribution as inhomogeneous boundary condition. The solution of the wave equation with respect to inhomogeneous boundary conditions is given by the Kirchhoff integral equation [15]. This principle states that SFS can be realized by a distribution of secondary monopole and dipole sources placed on the boundary ∂V of the listening area V which are driven by the directional gradient and the pressure of the sound field of the virtual source $S(\mathbf{x}, \omega)$, respectively. However, in practical implementations it is desirable to avoid the dipole secondary sources. A reasonable monopole only approximation of the Kirchhoff integral equation can be found by limiting the integration path and prescribing a convex secondary source

distribution. The driving function reads then [4]

$$D(\mathbf{x}_0, \omega) = 2a(\mathbf{x}_0) \frac{\partial}{\partial \mathbf{n}} S(\mathbf{x}_0, \omega), \quad (3)$$

where $\frac{\partial}{\partial \mathbf{n}}$ denotes the directional gradient evaluated at \mathbf{x}_0 and $a(\mathbf{x}_0)$ a window function that selects the active secondary sources. For simple virtual source models, e.g. plane waves and point sources, $a(\mathbf{x}_0)$ can be given in closed form using the acoustic intensity vector [20].

2.4. Three- and 2.5-dimensional Synthesis

From a physical point of view, the natural choice for the characteristics of the secondary sources is given by the according free-field Green's function. If V is a volume and ∂V the surface enclosing the volume, the secondary sources should have the characteristics of the three-dimensional free-field Green's function. Hence, the secondary source should act like an acoustic point source with monopole characteristics. This scenario is termed as three-dimensional synthesis. It has been shown that for a continuous secondary source distribution, three-dimensional synthesis can be realized without artifacts [7, 8].

However, due to technical constraints many practical realizations of SFS systems aim only at the synthesis in a plane using secondary sources placed on the boundary ∂V of the (planar) listening area V . In principle, this constitutes a two-dimensional problem and hence the two-dimensional free-field Green's function, which can be interpreted as the field produced by a line source positioned perpendicular to the target plane [15], is an appropriate choice for the secondary sources. Loudspeakers exhibiting the properties of acoustic line sources are not practical. Using point sources as secondary sources for the reproduction in a plane results in a dimensionality mismatch, therefore such methods are often termed as *2.5-dimensional synthesis*. It is well known from WFS, HOA and the SDM, that 2.5-dimensional reproduction techniques suffer from artifacts [3, 21, 8]. Most prominent are amplitude deviations between the desired virtual source and the synthesized sound field.

2.5. WFS and NFC-HOA

While NFC-HOA is based upon the explicit solution of the synthesis equation, WFS is based on an approximated implicit solution, as outlined above.

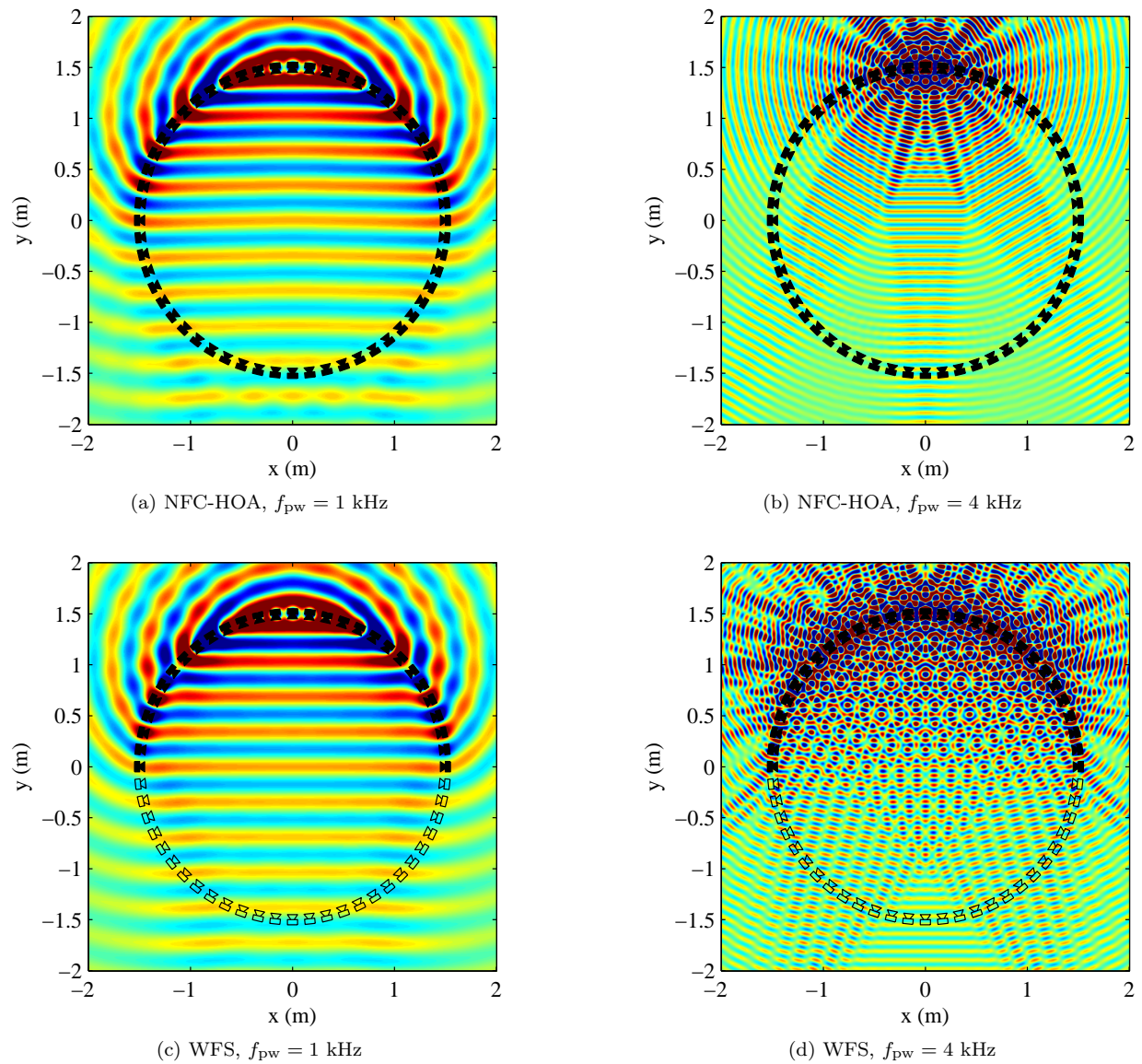


Fig. 2: 2.5-dimensional synthesis of a monochromatic plane wave using NFC-HOA (top row) and WFS (bottom row) using a circular distribution of secondary sources ($N = 56$, $R = 1.5$ m, $\alpha_{pw} = 270^\circ$). The active secondary sources are filled.

In order to briefly illustrate the properties of both approaches a sample scenario is presented here. An in-depth comparison can for instance be found in [22, 23]. The synthesis of a monochromatic plane wave using a circular array of $N = 56$ loudspeakers is considered as sample scenario. Figures 2a and 2b show the synthesized sound fields for NFC-HOA for two different frequencies. For the lower frequency (1 kHz) no spatial sampling artifacts are present and the desired plane wave is synthesized without major artifacts. The amplitude decay of the synthesized plane wave that can be observed is a consequence of 2.5-dimensional synthesis. However, for the higher frequency (4 kHz) shown in Figure 2b sampling artifacts are clearly visible. However, in a circular region in the center of the listening area almost no artifacts can be observed. The radius of this area decreases further with increasing frequency.

Figures 2c and 2d show the synthesized sound fields for WFS. Some deviations from the desired plane wave can be observed for the lower frequency (1 kHz). These are due to the approximations used in WFS to derive the implicit solution. For the higher frequency (4 kHz) sampling artifacts are clearly visible. In contrast to NFC-HOA shown in Figure 2b, the sampling artifacts of WFS are spread over the entire listening area.

3. LOCAL SOUND FIELD SYNTHESIS

3.1. Problem Statement

Traditional approaches to SFS, like WFS and NFC-HOA, aim at the accurate synthesis throughout the entire listening area V . Practical restrictions, especially the number of loudspeakers in current setups, pose limitations with respect to the frequency range the spatial structure of the desired sound field is preserved. This was illustrated in Figure 2.

In many situations an accurate synthesis in the entire listening area is not required. The potential listener positions are often restricted in practical situations like for instance in a car or living room environment. The goal of LSFS is to increase the accuracy within a limited (local) listening area, which is embedded in the traditional listening area V , at the cost of potential artifacts outside of the local listening area. Hence listeners located in the local listening area will benefit from the increased accuracy.

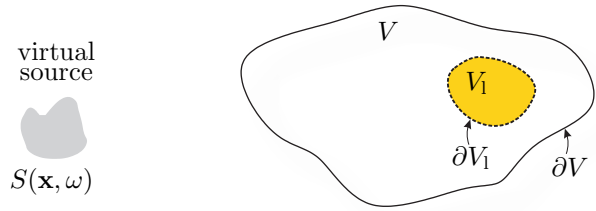


Fig. 3: Illustration of the geometry used to discuss the problem statement of local sound field synthesis.

Figure 3 depicts the geometry. The secondary sources are located on the border ∂V and should be driven such to synthesize the sound field $S(\mathbf{x}, \omega)$ of the virtual source accurately within the local listening area V_l with the boundary ∂V_l .

Several approaches have already been published which realize LSFS [10, 11, 12, 13, 14]. This paper introduces a novel approach that is based on virtual acoustic scattering and the principle of time-reversal in acoustics. The following two subsections introduce findings and theoretical foundations required for the novel approach introduced in Section 3.4.

3.2. Simple Source Formulation and Equivalent Scattering Problem

The simple source formulation, is based on constructing an acoustic scenario that results in a formulation of the synthesis equation that is equal to (4). However, it provides insights into the physical nature of the driving signal $D(\mathbf{x}, \omega)$.

We briefly outline the procedure discussed in [15]. Two equivalent but spatially disjoint radiation problems are constructed that are linked at the boundary ∂V . Both problems, the interior and exterior problem, are covered by the Kirchhoff integral equation. It is assumed that the sound pressure in the exterior region $S_-(\mathbf{x}, \omega)$ and in the interior region $S_+(\mathbf{x}, \omega)$ is continuous when approaching the boundary ∂V from the exterior or the interior, hence $S_+(\mathbf{x}, \omega) = S_-(\mathbf{x}, \omega)$ for $\mathbf{x} \in \partial V$. It is furthermore assumed that the normal derivatives are not continuous, hence $\frac{\partial}{\partial \mathbf{n}} S_-(\mathbf{x}_0, \omega) \neq \frac{\partial}{\partial \mathbf{n}} S_+(\mathbf{x}_0, \omega)$ for $\mathbf{x} \in \partial V$. This discontinuity of the normal derivatives represents the secondary source distribution. The simple

source formulation is then given as [15]

$$\oint_{\partial V} \left(\frac{\partial}{\partial \mathbf{n}} S_-(\mathbf{x}_0, \omega) - \frac{\partial}{\partial \mathbf{n}} S_+(\mathbf{x}_0, \omega) \right) G(\mathbf{x} - \mathbf{x}_0, \omega) dS_0 = \begin{cases} S_+(\mathbf{x}, \omega) & \text{for } \mathbf{x} \in V \\ S_+(\mathbf{x}, \omega) = S_-(\mathbf{x}, \omega) & \text{for } \mathbf{x} \in \partial V \\ S_-(\mathbf{x}, \omega) & \text{for } \mathbf{x} \notin V \cup \partial V \end{cases} \quad (4)$$

Comparison with (1) and having the problem statement of SFS in mind reveals that (4) provides an explicit expression for the driving signal $D(\mathbf{x}, \omega)$. However, computation of the driving signal requires knowledge of the exterior sound field $S_-(\mathbf{x}, \omega)$. Considering the equivalent scattering problem provides the required knowledge. In the following we will briefly outline the theory introduced in [16].

The first step is to assume that ∂V represents the boundary of a scattering object from which the sound field of the virtual source is scattered. The sum of the incidence field $S(\mathbf{x}, \omega)$ and the scattered field $P_s(\mathbf{x}, \omega)$, the total field $P_t(\mathbf{x}, \omega)$, is given as

$$P_t(\mathbf{x}, \omega) = S(\mathbf{x}, \omega) + P_s(\mathbf{x}, \omega). \quad (5)$$

Assuming homogeneous Dirichlet boundary conditions (aka pressure release or sound-soft boundary) on ∂V the total sound field vanishes $P_t(\mathbf{x}, \omega) = 0$ on the boundary ∂V ($\mathbf{x} \in \partial V$). According to (5), the scattered field $P_s(\mathbf{x}, \omega) = -S(\mathbf{x}, \omega)$ on the boundary ∂V ($\mathbf{x} \in \partial V$). Since the acoustic pressure is assumed to be continuous over the boundary ∂V and due to the uniqueness of the exterior radiation problem [15] we can conclude from (4) that $S_-(\mathbf{x}, \omega) = -P_s(\mathbf{x}, \omega)$ in the exterior region ($\mathbf{x} \notin V \cup \partial V$).

The considerations above allow for the following conclusions: (i) the driving signal for the secondary sources is given as the normal derivative of the total sound field and (ii) the sound field $S_-(\mathbf{x}, \omega)$ in the exterior region ($\mathbf{x} \notin V \cup \partial V$) of a sound field synthesis system equals the phase reversed field of the virtual source's sound field scattered at a virtual sound-soft object with the border ∂V .

3.3. The Time-Reversal Cavity

The inhomogeneous wave equation for a spatio-temporal Dirac shaped inhomogeneity is given as [15]

$$\nabla^2 p(\mathbf{x}, t) - \frac{1}{c^2} \frac{\partial^2}{\partial t^2} p(\mathbf{x}, t) = \delta(\mathbf{x} - \mathbf{x}') \delta(t), \quad (6)$$

where c denotes the speed of sound. The solution $p(\mathbf{x}, t)$ has to obey the initial and boundary conditions. Irrespectively of these, the solution of the wave equation (6) has the very interesting property that if $p(\mathbf{x}, t)$ is a solution of the wave equation (6), then $p(\mathbf{x}, -t)$ is also a solution. Since only second order derivatives with respect to space and time occur in the lossless wave equation, its solutions are invariant to a time-reversal. The major result of time-reversal acoustics is that the optimal way to focus acoustic waves on the initial source position \mathbf{x}' is a time-reversal of $p(\mathbf{x}, t)$ in the entire three-dimensional space. However, this theoretical concept cannot be applied in practice.

The concept of the time-reversal cavity [24] provides a practical solution by combining the principle of time-reversal acoustics with the Kirchhoff integral equation. This way the time-reversal in three-dimensional space is reduced to operations on a two-dimensional surface. Acoustic focusing in a time-reversal cavity consists of two steps: (i) recording and (ii) reconstruction.

In the first step, the acoustic pressure generated by the inhomogeneity at position \mathbf{x}' and the directional gradient of the acoustic pressure is recorded simultaneously on the surface $\mathbf{x}_0 \in \partial V$ enclosing the inhomogeneity. The inhomogeneity is removed for the second step, where secondary monopole and dipole sources are placed on the boundary ∂V . In the second step, the monopole sources are fed by the time-reversed directional gradient of the acoustic pressure and the dipoles by the time-reversed acoustic pressure recorded in the first step. To ensure causality a pre-delay should be introduced to the signals. The physical background of the time-reversal cavity and its properties have been discussed in [24], various acoustic focusing applications are presented e.g. in [25]. The time-reversal cavity does not only work for Dirac shaped inhomogeneities, it can also be applied to complex inhomogeneities.

The concept of the time-reversal cavity cannot be applied straightforwardly to SFS. This has two reasons: (i) for practical reasons we are seeking for a solution which requires only secondary monopole sources and (ii) although the time-reversal process produces optimal results with respect to focusing the acoustic energy, it cannot be applied straightforwardly to sound field synthesis since no care is taken about the

propagation direction of the traveling wave fronts. It has been shown in the context of synthesizing focused sources in WFS, that both problems can be overcome by a sensible selection of the active secondary sources [20, 26]. The technique can be understood as a far-field/high-frequency approximation of the Kirchhoff integral equation. A generalization of this principle is used in this paper.

3.4. Concept of Novel Approach

Section 3.2 revealed that the exterior sound field of a SFS system equals the phase reversed scattered field of the virtual source. Having in mind that the external radiation problem has a unique solution and considering the theory of the time-reversal cavity outlined in the previous subsection, it can be concluded that if we synthesize the scattered field at the boundary of the local listening area the sound field of the desired virtual source will be synthesized within the local listening area. Amongst others, this is a result of the simple source formulation (4).

As outlined in Section 3.2, the external sound field can be interpreted to emerge from the scattering of the virtual source at a sound soft scattering object. Hence, the external sound field can be interpreted to be the result of an inhomogeneity on ∂V_1 . When the directional gradient of the sound field is recorded, time-reversed and synthesized by secondary monopole sources, the desired sound field inside the virtual scattering object will result.

Combing the considerations given so far, the proposed technique is composed of the following steps:

1. compute the directional gradient of the sound field of the virtual source scattered by a virtual object that encloses the local listening area ∂V_1 ,
2. time-reverse the computed sound field,
3. select the required secondary sources, and
4. emit the time-reversed sound field by the active secondary sources.

As outline above, step 3 is required to control the propagation direction of the synthesized wave fronts. The following section derives driving functions for the proposed approach to LSFS.

3.5. Spherical/Cylindrical Local Listening Area

The proposed approach requires to compute the directional gradient of the sound field of the virtual source scattered by a virtual scattering object with the shape of the local listening area ∂V_1 . Analytic solutions to this problem exist only for rather simple geometries of the scattering object [27]. For other cases numerical methods like the finite element method (FEM) or the boundary element method (BEM) could be employed.

The following section derives the driving functions for the synthesis of a virtual plane wave with a cylindrical and spherical local listening area. Due to its height invariance, the cylindrical shape is the natural choice for two-dimensional scenarios and might also be suitable for 2.5-dimensional scenarios. The spherical shape is the natural choice for three dimensional synthesis and could also be assumed for 2.5-dimensional scenarios. The properties of both models for 2.5-dimensional synthesis are compared by the numerical simulations presented in Section 4.

For the discussion of the scattering at a cylinder the use of a cylindrical coordinate system is convenient. The transformation between the Cartesian and cylindrical coordinates is given as: $x = r \cos \alpha$, $y = r \sin \alpha$, $z = z$. Without loss of generality we assume that the listening area is located in the x - y -plane such that $z = 0$. The sound field $P_{\text{cyl},s}(\mathbf{x}, \omega)$ of a plane wave with incidence angle α_{pw} scattered by a sound-soft cylinder with radius a and infinite length located in the center of the coordinate system reads [28]

$$P_{\text{cyl},s}(\mathbf{x}, \omega) = - \sum_{n=-\infty}^{\infty} i^n \frac{J_n(\frac{\omega}{c}a)}{H_n^{(2)}(\frac{\omega}{c}a)} H_n^{(2)}(\frac{\omega}{c}r) e^{in(\alpha - \alpha_{\text{pw}})}, \quad (7)$$

where $J_n(\cdot)$ denotes the n -th order Bessel function and $H_n^{(2)}(\cdot)$ the n -th order Hankel function of second kind [29]. In practice, the infinite sum in (7) can be approximated by a finite series. According to [30], the number N of the secondary sources determines the degrees of freedom the sound field can exhibit within the local listening area. Hence, the sum can be truncated at $N' = \pm(N-1)/2$ for N being an odd number. Figure 4a illustrates the sound field scattered by a sound-soft cylinder for a monochromatic plane wave as incident sound field.

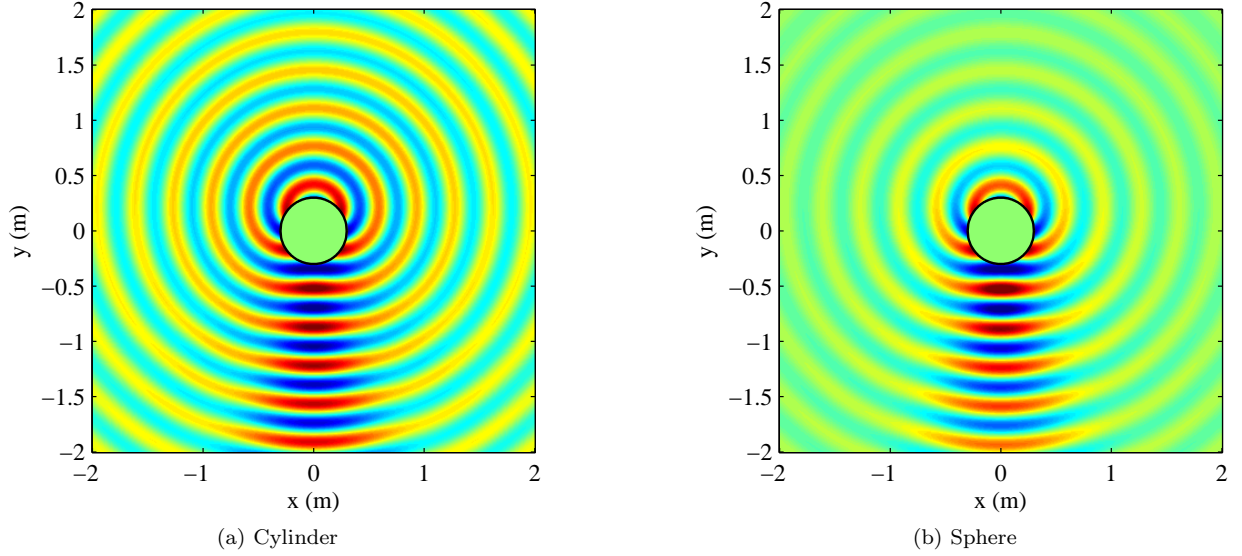


Fig. 4: Sound field scattered by a cylinder and a sphere with pressure release boundaries and radius $R = 0.3$ m for an incident monochromatic plane wave with frequency $f_{pw} = 1$ kHz and incidence angles $\theta_{pw} = 270^\circ$, $\phi_{pw} = 90^\circ$. The x - y -plane with $z = 0$ ($\beta = \pi/2$) is shown.

The scattering of a sphere is conveniently formulated in spherical coordinates. The transformation between the Cartesian and spherical coordinates is given as: $x = r \cos \alpha \sin \beta$, $y = r \sin \alpha \cos \beta$ and $z = r \cos \beta$, where α and β denote the azimuth and zenith angle, respectively. For 2.5-dimensional scenarios the listening area is assumed to be located in the x - y -plane without loss of generality, hence β is assumed to be $\beta = \pi/2$. The scattered sound field for a sound-soft sphere is given by [27]

$$P_{\text{sph},s}(\mathbf{x}, \omega) = -4\pi \sum_{n=0}^{\infty} \sum_{m=-n}^n i^n \frac{j_n(\frac{\omega}{c}a)}{h_n^{(2)}(\frac{\omega}{c}a)} h_n^{(2)}(\frac{\omega}{c}r) Y_n^m(\beta_{pw}, \alpha_{pw})^* Y_n^m(\beta, \alpha), \quad (8)$$

where $j_n(\cdot)$ denotes the n -th order spherical Bessel function, $h_n^{(2)}(\cdot)$ the n -th order spherical Hankel function of second kind, $Y_n^m(\cdot)$ the spherical harmonics of order n and degree m , β_{pw} the zenith angle of the incident plane wave and $(\cdot)^*$ denotes the complex conjugate of a quantity. Again the sum over n can be truncated with reasonable error. The number of elements required to provide computations with

a prescribed accuracy can be, in fact, evaluated rigorously. Several lemmas for bounds of the spherical Hankel functions can be found in [27]. Here we just require that $N > ka$ and selection of $N = lka$, with some $l > 1$ depending on the prescribed error provides accurate results.

For 2.5-dimensional synthesis $\beta_{pw} = \pi/2$ and the number of elements can be chosen equal to the case of the cylindrical scatterer discussed before. Figure 4b illustrates the sound field scattered by a spherical scatterer with pressure release boundaries. Only slight differences can be observed in comparison with Figure 4a showing the results for the cylinder.

The desired driving function for LSFS can be derived from equations (7) and (8) by computing the directional gradient of the sound pressure at the secondary source positions and applying the time-reversal principle together with a sensible selection of the secondary sources as

$$D(\mathbf{x}_0, \omega) = a(\mathbf{x}_0) \frac{\partial}{\partial \mathbf{n}} P_s(\mathbf{x}_0, \omega)^*, \quad (9)$$

where $a(\mathbf{x}_0)$ denotes a window function realizing the secondary source selection. Note the time reversal is

realized in the frequency domain by taking the complex conjugate of the sound field at the secondary source positions. A pre-delay has to be included in a practical realization in order to derive a causal driving function. The closed-form formulations of the window function $a(\mathbf{x}_0)$ derived in [20] for a focused source showed to work well also here. An additional spatial windowing (tapering) has furthermore provided good results in practice [3].

4. RESULTS

In the following, results from numerical evaluation of the proposed approach are presented. For practical reasons the properties of 2.5-dimensional local synthesis are discussed. Equation (9) has been evaluated numerically in MATLAB together with (1) in order to calculate the synthesized sound field. A point source model is used for the secondary sources. The directional gradient $\frac{\partial}{\partial \mathbf{n}} P_s(\mathbf{x}_0, \omega)$ of the scattered field has been derived analytically from (7) and (8) by calculating the gradient in cylindrical/spherical coordinates, performing a coordinate transformation to Cartesian coordinates and evaluating the scalar product with respect to the normal vector \mathbf{n} of the respective secondary source at position \mathbf{x}_0 .

In order to investigate the performance of the cylindrical and spherical model for the virtual scatterer, the same geometry as in Section 2.5 (cf. Figure 2) is chosen. A loudspeaker distribution with 56 loudspeakers arranged on a circle with radius of $R = 1.5$ m. The local listening area has a radius of $a = 0.3$ m and is positioned off-center by an offset of -0.3 m on the y -axis. The size has been chosen such to cover the size of a human head including some reasonable head movement. Figure 5a shows a global view of the synthesized sound field for a cylinder as virtual scatterer, while Figure 5b shows the same scenario for a sphere as scatterer. Both models are suitable for synthesizing a plane wave within the local listening area without major artifacts. Comparing both figures to figures 2b or 2d, where the same situation is shown for traditional WFS and NFC-HOA, reveals that the proposed approach is capable of increasing the accuracy within the local listening area. To allow for a better comparison of both models used for the virtual scatterer, figures 5c and 5d show a zoom into the local listening area. Both models show very similar performance,

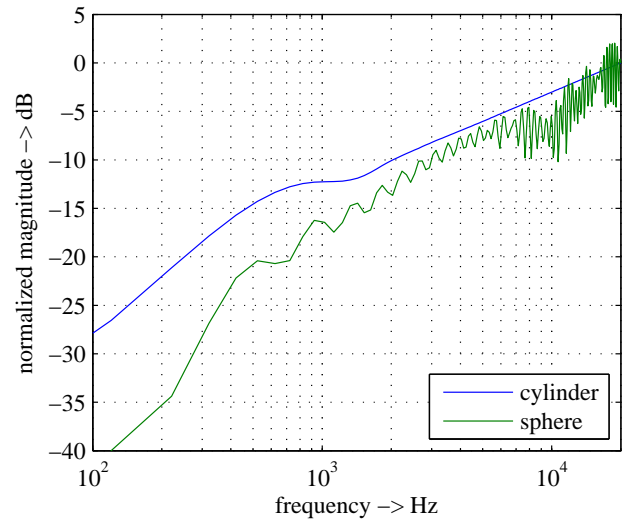


Fig. 6: Magnitude frequency response of LSFS in the center of the local listening area using a cylindrical and spherical virtual scatterer.

the spherical model is slightly better with respect to the spatial structure of the synthesized sound field.

It is well known from SFS that 2.5-dimensional synthesis has to be equalized by a pre-equalization filter [31]. Therefore the frequency response of both models used for the virtual scatterer is investigated. Figure 6 shows the magnitude frequency response in the center of the local listening area for a Dirac shaped plane wave as desired virtual source. The simulated scenario is the same as above (see Figure 5). It can be observed that both models do not result in a flat frequency response. The frequency response of the cylindrical scatterer exhibits two different slopes, a first one of approx. 6 dB/Octave and a second one with approx 3 dB/Octave. The transition frequency between the two slopes is about 1.5 kHz. The magnitude response is overall more complex for the spherical scatterer, however also here two different slopes can be observed below and above the same transition frequency. It can be concluded that the frequency response when using the cylindrical model as virtual scatterer can be compensated more easily by a pre-equalization filter. Hence, at the current state it seems to be preferable to use the cylindrical model.

One benefit of the proposed technique to LSFS is

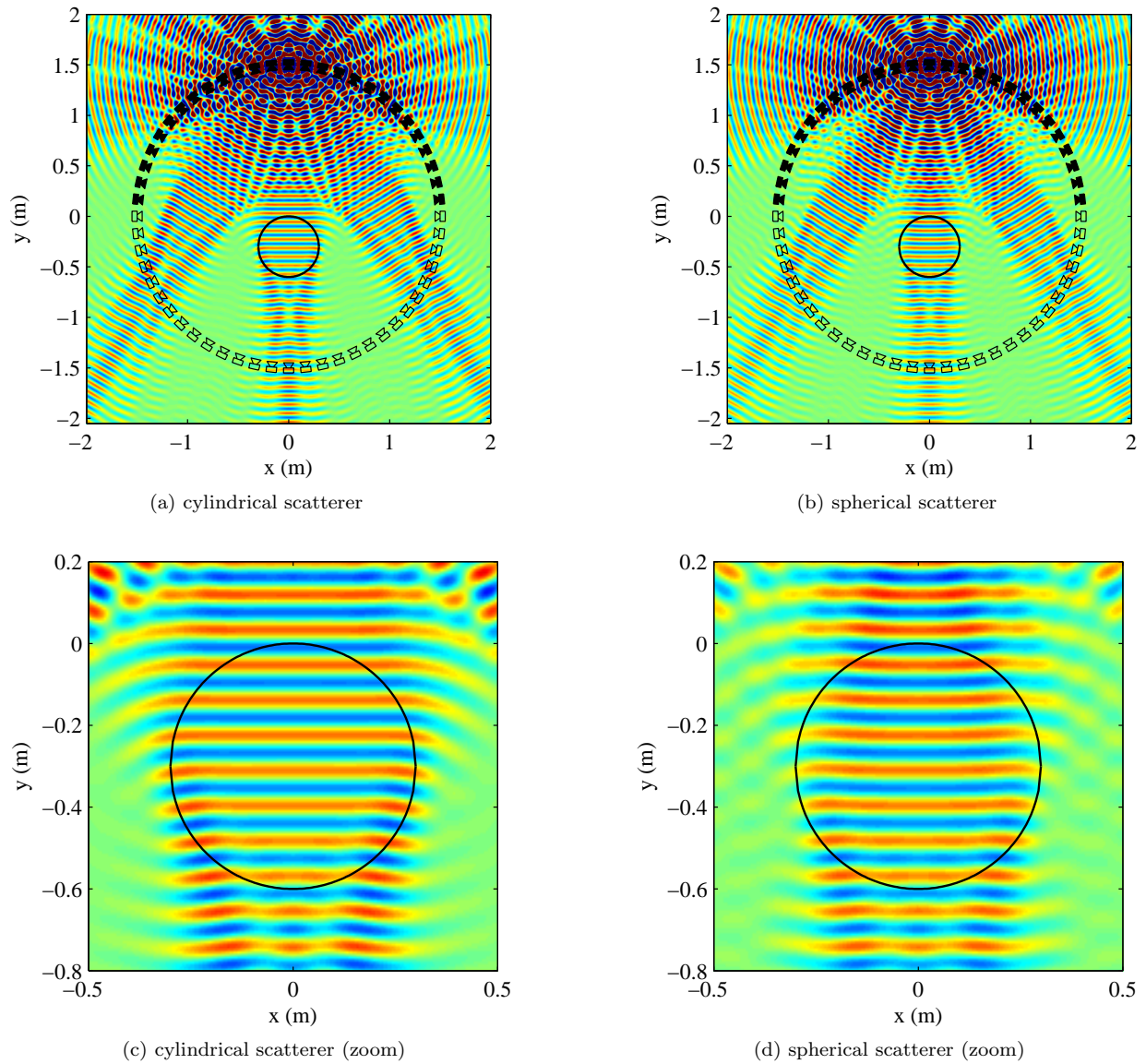


Fig. 5: Synthesized sound field using the proposed approach to LSFS with a circular loudspeaker array ($N = 56$, $R = 1.5$ m, $\alpha_{\text{pw}} = 270^\circ$, $f_{\text{pw}} = 4$ kHz, $a = 0.3$ m). The left row shows the results when using a cylindrical model for the scatterer, the right row a spherical model. A Hann window with a width of 30% from both sides of the active loudspeakers has been used for tapering. The active loudspeakers are filled.

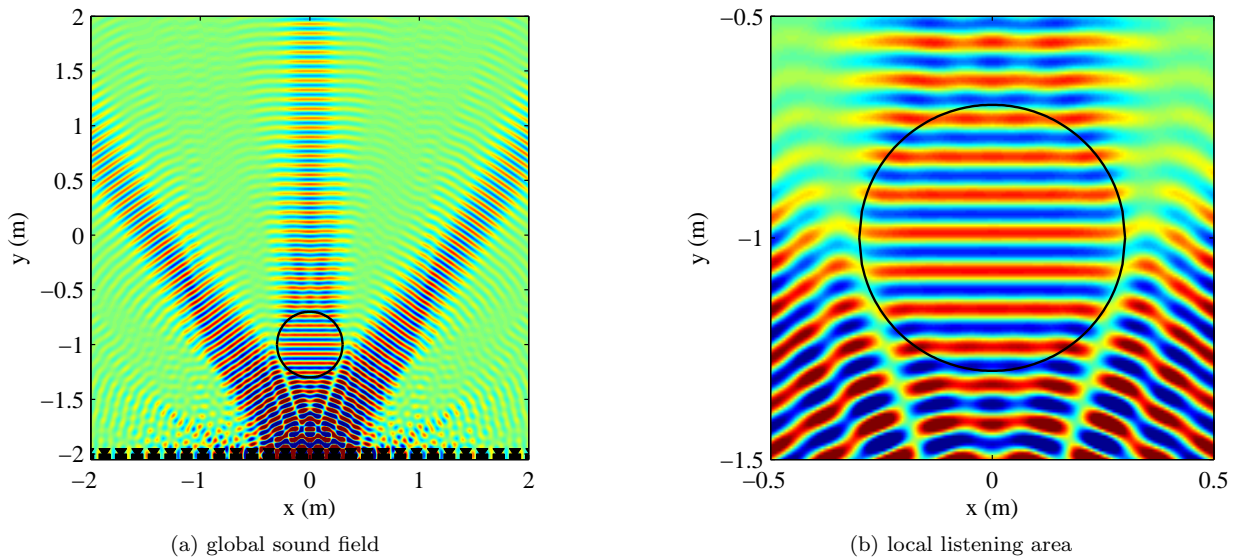


Fig. 7: Synthesized sound field using the proposed approach to LSFS with a linear loudspeaker array ($N = 40$, $\Delta x = 0.15$ m, $\alpha_{pw} = 90^\circ$, $f_{pw} = 4$ kHz, $a = 0.3$ m).

that it can be applied to almost arbitrary secondary source distributions. In order to illustrate this, a linear secondary source distribution is simulated. The scenario consists of a linear arrangement of $N = 40$ loudspeakers with a spacing of $\Delta x = 0.15$ m synthesizing a monochromatic plane wave with incidence angle $\alpha_{pw} = 90^\circ$ and frequency $f_{pw} = 4$ kHz. The aliasing frequency for this setup when driven by traditional WFS would be $f_{al} \approx 1140$ Hz [32]. Figure 7a shows a global view on the synthesized sound field and Figure 7b a zoom into the local listening area. Only minor artifacts can be observed within the local listening area, although the frequency of the synthesized plane wave is above the aliasing frequency of the array when driven with traditional WFS.

5. SUMMARY AND CONCLUSIONS

This paper presented a novel approach to local sound field synthesis. It is based upon the time-reversal principle and the use of a virtual acoustic scatterer with the shape of the local listening area. The sound field of the virtual source as scattered by the virtual scattering object is calculated at the secondary source positions, time-reversed and played back by selected secondary sources. Numerical simulations

of the synthesized sound field proved that the accuracy in terms of the upper frequency limit, up to which the synthesis is accurate, can be improved by a factor of 2-4 compared to conventional (non-local) synthesis for a restricted listening area covering approximately one person. For typical setups this results in an upper frequency limit of 4-10 kHz. However at the current state of knowledge it is not exactly clear what the requirements in terms of accuracy are for a human listener. The results presented in [9] indicate that the obtained accuracy could result in a higher perceptual quality than using traditional techniques.

The proposed approach allows for some interesting insights into the physical mechanisms of local sound field synthesis. The sound field between the local listening area and the secondary sources is given by the time-reversed sound field of the virtual source scattered by the local listening area. The sound fields synthesized by two other approaches we have published [10, 12] look quite similar to the results presented in this paper. Even so the derivation of the driving functions and the approximations used for each of the approaches are quite different. The theoretical background of SFS, as given in [16], shows

that the physical solution to the LSFS problem is unique. Hence when aiming at the physical synthesis of a virtual source within a local listening area these similarities between different approaches are not surprising. In this context it also interesting to compare Figures 5a or 5b to Figure 2b showing NFC-HOA. On first sight the results look very similar, however in the presented approach the location of the local listening area can be chosen freely.

The derivation of the proposed approach, as presented in this paper, is based upon the simple source approach and a virtual scatterer with pressure release boundaries. It is straightforward to extend the presented theory to rigid boundary conditions by reformulating the simple source approach (4) in terms of dipole secondary sources. Numerical simulations using rigid boundary conditions show very similar results as the ones presented in this paper. This topic will be investigated in more detail in the future.

The derivation of the driving function for 2.5-dimensional LSFS for the spherical local listening area is based on calculating the scattered sound field in the x - y -plane by setting $\beta = \pi/2$. An alternative approach to derive the driving function in 2.5-dimensional scenarios has been presented in [7]. Further work includes the application of this scheme to LSFS.

Although the synthesized sound fields in Figures 5 and 7 show a very promising performance, the proposed approach has to be evaluated in terms of broadband and perceptual properties. This will be performed in the future by investigating the synthesis of broadband virtual sources and listening experiments.

6. REFERENCES

- [1] F. Rumsey. *Spatial Audio*. Focal Press, 2001.
- [2] A.J. Berkhout, D. de Vries, and P. Vogel. Acoustic control by wave field synthesis. *Journal of the Acoustic Society of America*, 93(5):2764–2778, May 1993.
- [3] E.N.G. Verheijen. *Sound Reproduction by Wave Field Synthesis*. PhD thesis, Delft University of Technology, 1997.
- [4] S. Spors, R. Rabenstein, and J. Ahrens. The theory of wave field synthesis revisited. In *124th AES Convention*. Audio Engineering Society (AES), May 2008.
- [5] M.A. Gerzon. Width-height sound reproduction. *Journal of the Audio Engineering Society (JAES)*, 21:2–10, 1973.
- [6] J. Daniel. Spatial sound encoding including near field effect: Introducing distance coding filters and a viable, new ambisonic format. In *AES 23rd International Conference*, Copenhagen, Denmark, May 2003. Audio Engineering Society (AES).
- [7] J. Ahrens and S. Spors. Analytical driving functions for higher-order ambisonics. In *IEEE International Conference on Acoustics, Speech, and Signal Processing (ICASSP)*, Las Vegas, USA, April 2008.
- [8] J. Ahrens and S. Spors. Sound field reproduction using planar and linear arrays of loudspeakers. *IEEE Transactions on Audio, Speech and Language Processing*, 18(8):2038 – 2050, November 2010. doi:10.1109/TASL.2010.2041106.
- [9] H. Wittek. *Perceptual differences between wave-field synthesis and stereophony*. PhD thesis, University of Surrey, 2007.
- [10] J. Ahrens and S. Spors. An analytical approach to sound field reproduction with a movable sweet spot using circular distributions of loudspeakers. In *IEEE International Conference on Acoustics, Speech, and Signal Processing (ICASSP)*, Taipei, Taiwan, April 2009.
- [11] Y.J. Wu and T.D. Abhayapala. Spatial multi-zone soundfield reproduction. In *IEEE International Conference on Acoustics, Speech, and Signal Processing (ICASSP)*, Taipei, Taiwan, 2009.
- [12] S. Spors and J. Ahrens. Local sound reproduction by virtual secondary sources. In *AES 40th International Conference on Spatial Audio*, pages 1–8, Tokyo, Japan, October 2010. Audio Engineering Society (AES).

- [13] J. Hannemann and K.D. Donohue. Virtual sound source rendering using a multipole-expansion and method-of-moments approach. *Journal of the Audio Engineering Society (JAES)*, 56(6):473–481, June 2008.
- [14] E. Corteel, R. Pellegrini, and C. Kuhn-Rahloff. Wave field synthesis with increased aliasing frequency. In *124th AES Convention*, Amsterdam, The Netherlands, May 2008. Audio Engineering Society (AES).
- [15] E.G. Williams. *Fourier Acoustics: Sound Radiation and Nearfield Acoustical Holography*. Academic Press, 1999.
- [16] F.M. Fazi. *Sound Field Reproduction*. PhD thesis, University of Southampton, 2010.
- [17] J. Giroire. Integral equation methods for the helmholtz equation. *Integral Equations and Operator Theory*, 5(1):506–517, 1982.
- [18] F.M. Fazi, P.A. Nelson, J.E.N. Christensen, and J. Seo. Surround system based on three dimensional sound field reconstruction. In *125th AES Convention*, San Fransisco, USA, 2008. Audio Engineering Society (AES).
- [19] S. Spors and J. Ahrens. Towards a theory for arbitrarily shaped sound field reproduction systems. *Journal of the Acoustical Society of America*, 123(5):3930, May 2008.
- [20] S. Spors. Extension of an analytic secondary source selection criterion for wave field synthesis. In *123th AES Convention*, New York, USA, October 2007. Audio Engineering Society (AES).
- [21] J. Ahrens and S. Spors. An analytical approach to sound field reproduction using circular and spherical loudspeaker distributions. *Acta Acustica united with Acustica*, 94(6):988–999, December 2008.
- [22] S. Spors and J. Ahrens. A comparison of wave field synthesis and higher-order ambisonics with respect to physical properties and spatial sampling. In *125th AES Convention*. Audio Engineering Society (AES), October 2008.
- [23] J. Ahrens, H. Wierstorf, and S. Spors. Comparison of higher order ambisonics and wave field synthesis with respect to spatial discretization artifacts in time domain. In *AES 40th International Conference on Spatial Audio*, Tokyo, Japan, October 2010. Audio Engineering Society (AES).
- [24] D. Cassereau and Fink. M. Time-reversal of ultrasonic fields – part III: Theory of the closed time-reversal cavity. *IEEE Transactions on Ultrasonics, Ferroelectrics, and Frequency Control*, 39(5):579–592, Sept. 1992.
- [25] M. Fink. Time-reversed acoustics. *Scientific American*, pages 91–97, Nov. 1999.
- [26] S. Spors, H. Wierstorf, M. Geier, and J. Ahrens. Physical and perceptual properties of focused sources in wave field synthesis. In *127th AES Convention*. Audio Engineering Society (AES), October 2009.
- [27] N.A. Gumerov and R. Duraiswami. *Fast Multipole Methods for the Helmholtz Equation in three Dimensions*. Elsevier, 2004.
- [28] H. Teutsch. *Wavefield Decomposition using Microphone Arrays and its Application to Acoustic Scene Analysis*. PhD thesis, University of Erlangen-Nuremberg, 2005. <http://www.lnt.de/lms/publications> (last viewed on 4/16/2007).
- [29] M. Abramowitz and I.A. Stegun. *Handbook of Mathematical Functions*. Dover Publications, 1972.
- [30] H.M. Jones, A. Kennedy, and T.D. Abhayapala. On dimensionality of multipath fields: Spatial extent and richness. In *Proc. Int. Conf. Acoustics, Speech, and Signal Processing (ICASSP 02)*, Orlando, USA, May 2002.
- [31] S. Spors and J. Ahrens. Analysis and improvement of pre-equalization in 2.5-dimensional wave field synthesis. In *128th AES Convention*, pages 1–17, London, UK, May 2010. Audio Engineering Society (AES).
- [32] S. Spors and R. Rabenstein. Spatial aliasing artifacts produced by linear and circular loudspeaker arrays used for wave field synthesis.

In *120th AES Convention*, Paris, France, May
2006. Audio Engineering Society (AES).